Geoscientific
Instrumentation
Methods and
Data Systems

Digital photography for assessing the link between vegetation phenology and CO_2 exchange in two contrasting northern ecosystems

Maiju Linkosalmi[1], Mika Aurela[1], Juha-Pekka Tuovinen[1], Mikko Peltoniemi[2], Cemal M. Tanis[1], Ali N. Arslan[1], Pasi Kolari[3], Kristin Böttcher[4], Tuula Aalto[1], Juuso Rainne[1], Juha Hatakka[1], and Tuomas Laurila[1]

[1]Finnish Meteorological Institute, Helsinki, Finland
[2]Natural Resources Institute Finland (LUKE), Vantaa, Finland
[3]Faculty of Biosciences, University of Helsinki, Helsinki, Finland
[4]Finnish Environment Institute (SYKE), Helsinki, Finland

Correspondence to: Maiju Linkosalmi (maiju.linkosalmi@fmi.fi)

Abstract. Digital repeat photography has become a widely used tool for assessing the annual course of vegetation phenology of different ecosystems. By using the green chromatic coordinate (GCC) as a greenness measure, we examined the feasibility of digital repeat photography for assessing the vegetation phenology in two contrasting high-latitude ecosystems. Ecosystem–atmosphere CO_2 fluxes and various meteorological variables were continuously measured at both sites. While the seasonal changes in GCC were more obvious for the ecosystem that is dominated by annual plants (open wetland), clear seasonal patterns were also observed for the evergreen ecosystem (coniferous forest). Daily and seasonal time periods with sufficient solar radiation were determined based on images of a grey reference plate. The variability in cloudiness had only a minor effect on GCC, and GCC did not depend on the sun angle and direction either. The daily GCC of wetland correlated well with the daily photosynthetic capacity estimated from the CO_2 flux measurements. At the forest site, the correlation was high in 2015 but there were discernible deviations during the course of the summer of 2014. The year-to-year differences were most likely generated by meteorological conditions, with higher temperatures coinciding with higher GCCs. In addition to depicting the seasonal course of ecosystem functioning, GCC was shown to respond to environmental changes on a timescale of days. Overall, monitoring of phenological variations with digital images provides a powerful tool for linking gross primary production and phenology.

1 Introduction

Phenology is an important factor in the ecology of ecosystems. The most distinctive phenomena comprising vegetation phenology are the changes in plant physiology, biomass and leaf area (Migliavacca et al., 2011; Sonnentag et al., 2011, 2012; Bauerle et al., 2012). In part, these changes drive the carbon cycle of ecosystems, and they have various feedbacks to the climate system through effects on surface albedo and aerodynamic roughness, and ecosystem–atmosphere exchanges of various gases (e.g. H_2O, CO_2 and volatile organic compounds) (Arneth et al., 2010). Besides leaf area, gas exchange is modulated by seasonal variations in photosynthesis and respiration (Richardson et al., 2013). Globally, these variations contribute to the fluctuations in the atmospheric CO_2 concentration (Keeling et al., 1996). In the long term, possible trends in vegetation phenology can have a systematic effect on the mean CO_2 level. Phenology further plays a role in the competitive interactions, trophic dynamics, reproductive biology, primary production and nutrient cycling (Morisette et al., 2009). Phenological phenomena are largely controlled by abiotic factors such as temperature, water availability and day length (Bryant and Baird, 2003; Körner and

Basler, 2010), and thus they are sensitive to climate change (Richardson et al., 2013; Rosenzweig et al., 2007; Migliavacca et al., 2012).

Several studies have reported an advanced onset of the growing season during recent decades (Linkosalo et al., 2009; Delbart et al., 2008; Nordli et al., 2008; Pudas et al., 2008). An earlier onset of growth has been observed to play a significant role in the annual carbon budget of temperate and boreal forests, while lengthening autumns have a less clear effect (Goulden et al., 1996; Berninger, 1997; Black et al., 2000; Barr et al., 2007; Richardson et al., 2009). This can be explained by the rapid C accumulation that starts as soon as conditions turn favourable for photosynthesis and growth in spring, while the opposing effect, i.e. ecosystem respiration, becomes increasingly important in summer and autumn (White and Nemani, 2003; Dunn et al., 2007).

In general, monitoring of vegetation changes by digital cameras has become feasible with the development of advanced but inexpensive cameras that produce automated and continuous real-time data. It has been shown that simple time-lapse photography can facilitate detection of vegetation phenophases and even the related variations in CO$_2$ exchange (Wingate et al., 2015; Richardson et al., 2007, 2009). This provides new possibilities for monitoring and modelling of ecosystem functioning, for verification of remote sensing products, and for analysis of ecosystem CO$_2$ exchange fluxes and related balances. Especially dynamic vegetation models and simulations of C cycle could be improved by more accurate information on the timing of budburst and leaf senescence, as simple empirical parameterizations, typically based on degree days or the onset and offset dates of C uptake, are presently used as indicators of the growing season start and end (Baldocchi et al., 2005; Delpierre et al., 2009; Richardson et al., 2013).

Digital cameras produce red-green-blue (RGB) colour channel information, from which different greenness indices can be calculated. For example, canopy greenness has been expressed in terms of the so-called green chromatic coordinate (GCC), which has been related to vegetation activity and further to carbon uptake of forests (Richardson et al., 2007, 2009; Ahrends et al., 2009; Ide et al., 2011) and peatlands (Sonnentag et al., 2011; Peichl et al., 2015). In deciduous forests, the main driver of gas exchange is leaf area that changes rapidly in spring and autumn, which is easy to detect. In evergreen conifer forests the leaf area changes are much smaller, so it is not obvious whether a similar relationship can be established for them. In a peatland environment, repeat images have been used to map the mean greenness of mire vegetation over a wide area (Peichl et al., 2015). For peatland ecosystems with a heterogeneous vegetation cover, it may be possible to simultaneously detect seasonality effects of different vegetation types. Thus digital repeat images of differentially developing vegetation types could potentially help decompose an integrated CO$_2$ flux observation into components allocated to these vegetation types.

Comparisons of phenological observations made in contrasting ecosystems are needed for highlighting the phenological features that can be extracted from camera monitoring at different sites (Wingate et al., 2015; Keenan et al., 2014; Toomey et al., 2015; Sonnentag et al., 2012). Differences in the ecosystem characteristics may also affect the ideal set-up of cameras and the interpretation of images, for example in conjunction with surface flux data.

The objectives of this study were to (1) evaluate the digital repeat photography as a method for monitoring the phenology of boreal vegetation at high latitudes, (2) investigate the differences in the phenology between two adjacent but contrasting ecosystems (pine forest and wetland) located in northern Finland, and (3) assess whether the data obtained from such cameras can support the interpretation of the micrometeorological measurements of CO$_2$ fluxes conducted at the sites.

This paper is structured as follows: Sect. 2 introduces the measurement sites, camera set-up, image analysis, and the CO$_2$ flux and meteorological data employed; Sect. 3 provides the results and related discussion, including tests of the monitoring system and an analysis of the observed phenological development in relation to CO$_2$ exchange; finally, Sect. 4 presents the conclusions emerging from this study.

2 Materials and methods

2.1 Measurement sites

The study sites were located at Sodankylä in northern Finland, 100 km north of the Arctic Circle. They represent two contrasting ecosystems, a Scots pine (*Pinus sylvestris*) forest (67°21.708′ N, 26°38.290′ E; 179 m a.s.l.) and an open pristine wetland (67°22.117′ N, 26°39.244′ E; 180 m a.s.l.). The long-term (1981–2010) mean temperature and precipitation within the area are −0.4 °C and 527 mm, respectively (Pirinen et al., 2012).

The Scots pine stand is located on fluvial sandy podzol and has a dominant tree height of 13 m and a tree density of 2100 ha^{-1}. The age of the trees within the camera scope is about 50 years. A single-sided leaf area index (LAI) of 1.2 m^2 m^{-2} has been estimated for the stand based on a forest inventory in 2000. The sparse ground vegetation consists of lichens (73 %), mosses (12 %) and ericaceous shrubs (15 %).

The wetland site is located on a mesotrophic fen that represents typical northern aapa mire. The vegetation at this site mainly consists of low species (*Carex* spp., *Menyanthes trifoliata*, *Andromeda polifolia*, *Betula nana*, *Vaccinium oxycoccos*, *Sphagnum* spp.). There are no tall trees, only some *B. pubescens* and a few isolated Scots pines. Different types of vegetation are located on drier (strings) and wetter (flarks) parts of the wetland.

The physical surface structure (aerodynamic roughness length) differs between the pine forest and wetland sites.

Also, the microclimate and surface exchange of CO_2 and sensible and latent heat differ due to different vegetation and soil characteristics.

2.2 Camera set-up

The images analysed in this study were taken automatically with StarDot Netcam SC 5 digital cameras. The set-up included a weather-proof housing and connections to line current and a web server. The pictures were stored in the 8 bit JPEG format every 30 min with 2592 × 1944 resolution and transferred automatically to a remote server. The daily collecting period varied according to the time of the year roughly covering the daylight hours.

At the forest site, the cameras were mounted to a tower at two different heights: 29 m ("canopy camera") and 13 m ("crown camera"). The viewing angle of the canopy camera was 45° from the horizontal plane, while the crown camera was positioned nearly horizontally. The images of the canopy camera covered parts of the forest canopy and some general landscape. The crown camera was focused to individual trees to detect their phenological development (e.g. bud burst, shoot growth, needle shedding) more closely. At the wetland site, the camera was adjusted in an angle of 45° on top of a 2 m pole. This camera mostly observed the ground vegetation, with some *B. pubescens* and sky also visible in the images. All cameras were placed facing the north to minimize lens flare and maximize illumination of the canopy.

2.3 Grey reference plates

At the forest site, grey reference plates were employed to monitor the stability of the image colour channels. The plates were attached to the cameras in such a way that they are visible in every picture. The idea behind the reference plates was to detect possible day-to-day shifts in the colour balance due to changing weather conditions, such as radiation variations. The reference images should also not show any obvious seasonality (Petach et al., 2014). The grey colour of the plates was close to the "true grey" in a sense that it has an equal mix of red, green and blue colour components. To achieve this, the reference plates were painted with Tikkurila grey/1948 (RGB values: R = 95, G = 95, B = 95).

2.4 Automatic image analysis

The digital images were analysed with the FMIPROT software that has been designed as a toolbox for image processing for phenological and meteorological purposes (Tanis and Arslan, 2016). FMIPROT calculates the colour fractions for red, green and blue channels. In the present analysis we use the GCC defined as

$$GCC = \frac{\sum G}{\sum R + \sum G + \sum B},$$ (1)
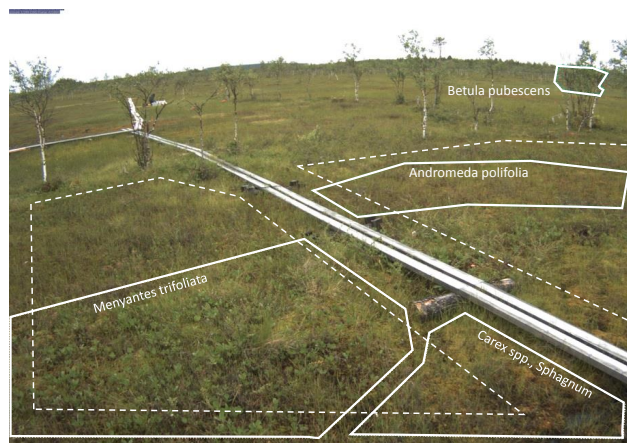

Figure 1. View from the wetland camera. The solid lines indicate four regions of interest defined according to vegetation types. The dashed lines indicate the region of interest that includes all vegetation types except *Betula pubescens*.

where $\sum G$, $\sum R$ and $\sum B$ are the sums of green, red and blue channel digital numbers, respectively, of all pixels comprising an image.

Within each image, it was possible to define limited subareas of regions of interest (ROIs). The ROI feature of FMIPROT makes it possible to limit the GCC calculation to an area that represents a homogeneous vegetation area. It also provides an option for analysing several subareas within the image simultaneously.

2.5 Selection of the region of interest

At the wetland site, GCC was calculated separately for four different, clearly identifiable vegetation types. These vegetation types were dominated by (1) bog rosemary (*Andromeda polifolia*) and other shrubs, (2) sedges (*Carex* spp.) and *Sphagnum* mosses, (3) big-leafed bogbean (*Menyanthes trifoliate*), and (4) downy birch (*Betula pubescens*) (Fig. 1). The first three ROIs also included other ground vegetation, while the fourth ROI was limited to the birch canopy. The GCC values were also analysed from a larger area that includes the three first vegetation types (Fig. 1).

The forest site had two cameras, one zoomed to the crown of a pine tree (Fig. 2) and the other providing a general view of the canopy (Fig. 3). From the general canopy image, three separate ROIs were subjectively selected with an aim to define similar homogenous areas of forest canopy (Fig. 3).

2.6 CO_2 flux measurements

The ecosystem–atmosphere CO_2 exchange was measured at both study sites by the micrometeorological eddy covariance (EC) method. The EC measurements provided continuous data on the CO_2 fluxes averaged on an ecosystem scale. The vertical CO_2 flux is obtained as the covariance of the

Figure 2. View from the pine forest crown camera. The line indicates the region of interest.

Figure 3. View from the pine forest canopy camera. The lines indicate three regions of interest.

high-frequency (10 Hz) fluctuations of vertical wind speed and CO_2 mixing ratio (Baldocchi, 2003). At both sites, the EC measurement systems consisted of a USA-1 (METEK GmbH, Elmshorn, Germany) three-axis sonic anemometer/thermometer and a closed-path LI-7000 (LI-COR, Inc., Lincoln, NE, USA) CO_2/H_2O gas analyzer. The measurement systems and the data processing procedures have been presented in detail by Aurela et al. (2009).

The CO_2 fluxes obtained from the EC measurements represent the net ecosystem exchange (NEE) of CO_2, which is the sum of gross photosynthetic production (GPP) by plants and a respiration term that includes both the autotrophic respiration by plants and the heterotrophic respiration by microbes. GPP is typically derived from the NEE data by using a dedicated flux partitioning technique, for example based on nonlinear regressions with photosynthetic photon flux density (PPFD) and air temperature as predictors (Reichstein et al., 2005). Instead of performing such an explicit partitioning, we determined the daily GPP in terms of the gross photosynthesis index (GPI); for details, see Aurela et al. (2001), where a similar index was termed "PI". GPI indicates the maximal photosynthetical activity in optimal radiation conditions. It is obtained by calculating the differences of the daily averages of the daytime (PPFD $> 600 \, \mu\mathrm{mol\,m^{-2}\,s^{-1}}$, which limit represents light saturation of photosynthesis at our sites) and night-time (PPFD $< 20 \, \mu\mathrm{mol\,m^{-2}\,s^{-1}}$) NEE. The resulting GPI scales well with the maximal GPP obtained from a traditional NEE partitioning, despite the day–night differences in respiration. GPI provides a useful measure especially for depicting the seasonal GPP cycle, but as it is robust against missing data, it also estimates photosynthetic activity during fast changes due to short-term variations in air temperature and humidity (Aurela et al., 2001).
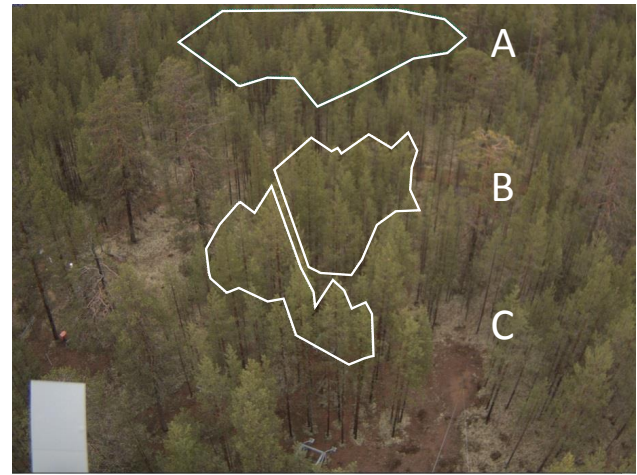
2.7 Meteorological measurements

An extensive set of supporting meteorological variables was measured at both measurement sites, including air temperature and humidity, various soil parameters (temperature, humidity, soil heat flux and water table level) and different radiation components (incoming and outgoing shortwave (SW) radiation, PPFD and net radiation). Here we used the temperature data measured at 3 m height on the wetland (Vaisala, HMP155D) and at 8 m at the forest site (Pentronic, PT100). From the SW radiation measurements (Kipp & Zonen, CM11) we calculated the surface albedo as the proportion of incident radiation that is reflected back to the atmosphere by the underlying surface. In addition, fractional cloud cover (CL) data were available from the nearby observatory.

3 Results and discussion

3.1 Testing the set-up

3.1.1 Effect of environmental conditions on GCC

An accurate GCC observation requires a sufficient illumination level, which was here ensured by selecting only mid-day (10:00–14:00 local winter time) photographs for further analysis. This period was determined on the basis of the GCC of the grey reference plate in different radiation conditions (Supplement, Figs. S1–S3).

The influence of cloudiness on GCC was estimated from the data collected in July 2014. This particular month was selected for the test because July represents the peak growing season (for both radiation levels and LAI), and in July 2014 sunny and cloudy days were equally frequent. Based on the observations of fractional cloud cover (rang-
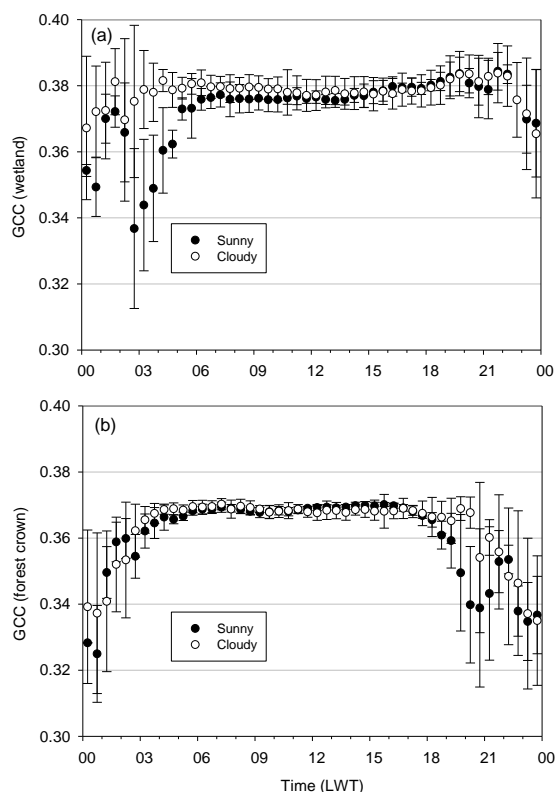
Figure 4. Mean ($\pm$ standard deviation shown by error bars) diurnal cycle of GCC during sunny and cloudy conditions observed with **(a)** the tree crown and **(b)** the wetland cameras in July 2014.

Figure 5. Mean daytime (10:00–14:00, local winter time) GCC of different regions of interest (vegetation types) during the measurement period of May 2014 to October 2015. Wetland refers to combined ROI shown in Fig. 5b. The grey circles indicate the wintertime data that are influenced by an insufficient light level.

and July), the difference was less than 10 % of the seasonal variation.

3.1.2 Sensitivity of GCC to selection of the region of interest

The sensitivity of the GCC values to the selection of a sub-area within an image, i.e. a region of interest, was tested by comparing the GCC calculated for different vegetation patches. In particular, we wanted to examine, on the one hand, whether the forest images are homogeneous and thus insensitive to the ROI definition; on the other hand, the wetland images may provide an opportunity to simultaneously observe various microecosystems incorporated into a single image.

The GCC values of the wetland ROIs defined according to vegetation types showed significant differences in the seasonal cycle, both in the timing of the major changes in spring and autumn and in the magnitude of the maximum GCC (Fig. 5). For example, downy birch had the earliest growth onset, while the big-leafed bogbean had the largest growing-season maximum. While the seasonal patterns of the GCCs of different ROIs can be compared, the same may not be true for the absolute GCC values, which were affected by different viewing angles and distances to the target. To gain a better insight into the quantitative differences between different ROIs, these ROI-specific GCC data should be investigated in conjunction with direct vegetation analysis (LAI, biomass) and small-scale (chamber-based) CO$_2$ exchange measurements. For further analysis here we chose to use the larger ROI combining three vegetation types (Fig. 1), which matches better the areally integrating flux measurements.

The daily mean GCC values of different forest canopy ROIs remained very similar throughout the time series (Fig. 6). The GCC values determined from crown images differed from those from the camera with a general canopy view, most likely because the cameras had different viewing

ing from clear sky with CL $= 0$ to completely cloudy conditions with CL $= 8$), the images were pooled to two contrasting cloudiness groups representing sunny (CL $= 0$–1) and cloudy (CL $= 7$–8) conditions. During the daily period of 10:00–14:00, the differences in the mean GCC between sunny and cloudy conditions were statistically insignificant (Mann–Whitney U test) (Fig. 4). The mean GCC difference between the cloudy and sunny groups was 0.0014 and 0.0011 for the fen and forest, respectively. Sonnentag et al. (2012) found an equivalently small, though in part statistically significant, difference between the diurnal GCC cycles of sunny and overcast situations for their deciduous and coniferous forests.

The dependence of GCC on the solar angle with respect to ROI was also estimated from the data of July 2014 (Fig. 4). The difference between the minimum and maximum values of the hourly GCC means within the daytime window was 0.0030 and 0.0020 for sunny and cloudy cases, respectively. This is less than 5 % of the seasonal amplitude of the GCC curve (0.069 between May and July) associated with phenological greening of the fen. At the forest site, the corresponding values were 0.0022 (sunny) and 0.0012 (cloudy) and, despite the lower annual amplitude (0.024 between May
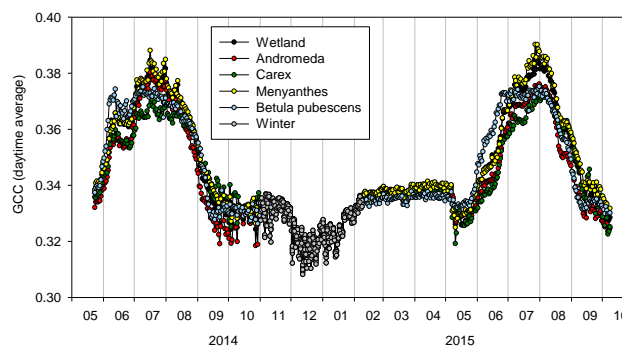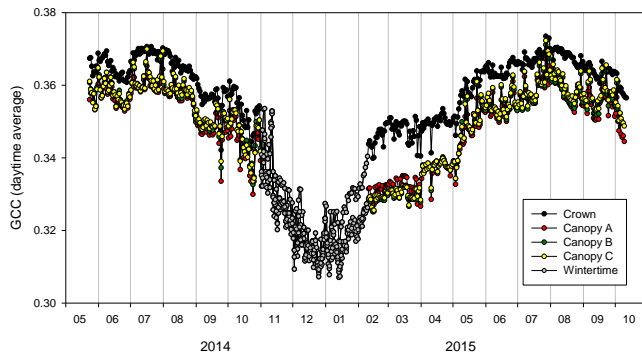
Figure 6. Mean daytime (10:00–14:00, local winter time) GCC values of different ROIs from two forest cameras during the measurement period of May 2014 to October 2015. The grey circles indicate the wintertime data that are influenced by an insufficient light level.

angles and distances to the object. The contribution of ground is mixed with the canopy signal, which partially explains why the GCC values in the distant canopy camera images were lower than in the crown camera images. In winter, there was more snow visible behind the canopy in the smaller-scale ROIs. Thus, we decided on using in further analysis only the images from the crown camera.

3.2 Phenological development

3.2.1 Wetland site

As previously observed by Peichl et al. (2015), at the wetland the growing season is clearly discernable in the development of GCC data (Fig. 7). GCC started to increase as soon as the wetland vegetation started to assimilate CO$_2$. This growth onset took place in May after the snowmelt, for which the ground albedo provides a sensitive indicator by quantifying the proportion of incident solar radiation that is reflected back to the atmosphere. However, the onset was preceded by a short period of reduced GCC values, which were associated with the moist and dark soil.

The warm spells during late May and early June in 2014 induced a rapid emergence and growth of annual plants. Despite the later snowmelt that year, by mid-June the growing season had developed much further than in 2015. This difference is clearly visible in the GCC as well as photosynthetic activity (GPI) data (Fig. 7). The cold period in late June 2014 ceased this fast development, which is also well reflected in the GCC data that show a stabilization and even a temporary reduction during that period. GPI shows a similar pattern, highlighting the coherence between the greenness observation and the actual photosynthetic processes.

Following the earlier onset of the growing season in 2014, the peak of plant development was also observed earlier (Fig. 7). However, the magnitude of the GCC maxima during the two years was the same (0.385). From mid-August
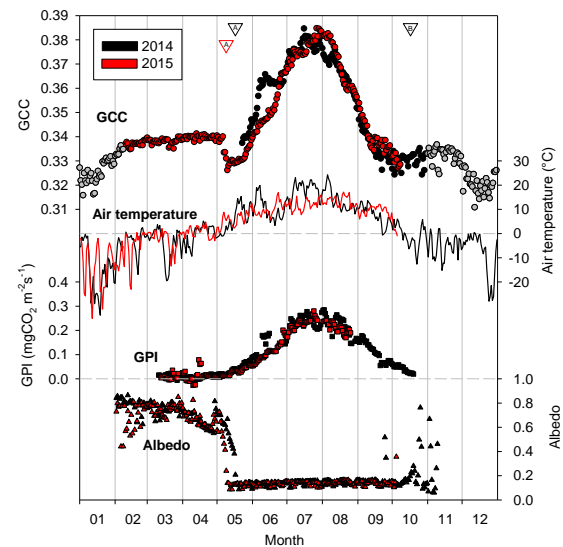

Figure 7. Mean daytime (10:00–14:00, local winter time) GCC (of the ROI shown in Fig. 1b) together with the daily mean air temperature, gross photosynthesis index (GPI) and albedo in 2014–2015 at the wetland site. The triangles indicate the dates of snowmelt (A) and snow appearance (B). The grey circles indicate the wintertime data that are influenced by an insufficient light level.

to mid-September, the rate of GCC decline was approximately the same in 2014 and 2015. In mid-September, the slightly higher GCC in 2014 can be attributed to a warm period. By the first sub-zero values in daily mean temperatures, the GCC had decreased to its minimum value, close to the springtime minimum, and by the snowfall in mid-October it had started increasing towards the level observed for the fully snow-covered conditions in spring.

Previous observations suggest that GPP is well correlated with the GCC of wetlands, especially during spring (Peichl et al., 2015). Our results support these observations showing a strong relationship between the daily GCC and GPI data (Fig. S4), with a correlation coefficient of 0.90 and 0.92 for the snow-free period in 2014 and 2015, respectively. Especially during the springtime, the match between the GCC and GPI time series was remarkably close during both years, while in the autumn of 2014 GPI lagged slightly behind GCC.

3.2.2 Forest site

Due to the closeness of the measurement sites, the meteorological conditions in forest were similar to those observed at the wetland (Figs. 7 and 8). However, the onset of photosynthetical activity differed slightly at the beginning of the growing season: the warm days of early May 2015 were not observed at the wetland as an GPI increase due to the absence of annual vegetation right after the snowmelt, while the photosynthesis of boreal trees is triggered as soon as temperature
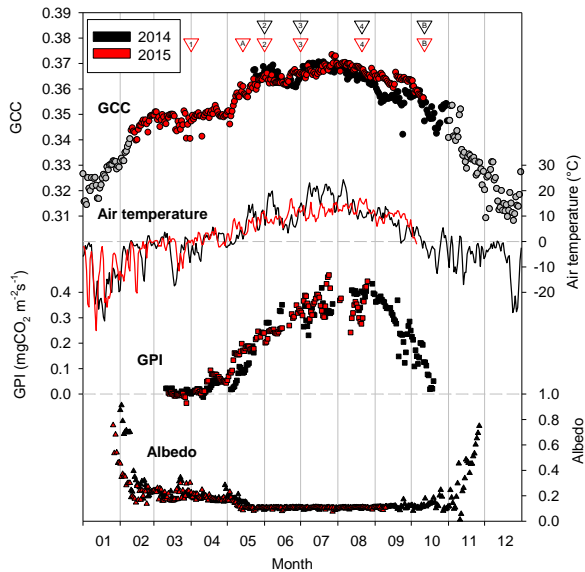
Figure 8. Mean daytime (10:00–14:00, local winter time) GCC (crown camera) together with the daily mean air temperature (at 18 m), gross photosynthesis index (GPI) and albedo in 2014–2015 at the forest site. The triangles indicate the start dates of visually observed phenological phases (1 – bud burst, 2 – bud growth, 3 – shoot growth, 4 – old needle browning) and snow status (A – snowmelt, B – snow appearance). The grey circles indicate the wintertime data that are influenced by an insufficient light level.

reaches a sufficient level (Tanja et al., 2003). Thus the growing season in the forest started earlier in 2015 than in 2014, while that was not the case at the wetland. Nevertheless, the warm period in late May–early June 2014 also enhanced the forest growth, and by mid-June both GCC and GPI had surpassed the corresponding level in 2015. The cold period in late June 2014 was again observed as reduced CO_2 uptake and even a clearer reduction in GCC than at the wetland.

Although in deciduous forest and open wetlands GCC is generally well correlated with the gross ecosystem photosynthesis during the start of the growing season (Peichl et al., 2015; Toomey et al., 2015), for evergreen needleleaf forests it has been reported that such correlation is often weaker (Toomey et al., 2015; Wingate et al., 2015). In our pine forest, however, the simultaneous development of GCC and photosynthesis was evident during the year with spring data available (Fig. S5).

Similarly to the wetland, the maximum GCC level at the forest site did not differ between 2014 and 2015, but this level was reached slightly earlier in 2014. This was probably due to the higher temperatures during the first part of the growing season. During both years, GCC started decreasing at the same time, i.e. at the end of July. This was slightly earlier than the start of the senescence detected visually (Phase 4 in Fig. 8). Similarly to the wetland, in 2014 there was a clear phase difference between GCC and GPI, the latter of which

stayed at the maximum level until the end of August. In forest, this may be due to the oldest needles, whose senescence takes place in August, while their photosynthetic capacity has diminished already earlier (Vesala et al., 2005).

In both 2014 and 2015, the photosynthetic activity continues until the end of August, but the interannual comparison is not possible here owing to the missing CO_2 data in 2015. Nevertheless, in both years GCC decreases to the wintertime level at the beginning of October, at the same time as the daily mean temperature decreases below 0 °C.

Our results show that the phenological development of the pine canopy could be accurately monitored with the GCC analysis, even though the GCC changes in forest were subtler than those observed for the wetland vegetation. This was confirmed by visually identifying the phenological stages of the forest from the crown camera pictures (Fig. 8). In 2014, the cameras were installed too late to detect the bud burst, but the GCC time series was consistent with the observation that the buds started their growth at the beginning of June and remained brown until the beginning of July, when they started to green.

4 Conclusions

We demonstrated the feasibility of digital repeat photography for assessing the link between vegetation phenology and CO_2 exchange for two contrasting high-latitude ecosystems. While the seasonal changes in the greenness index GCC are more obvious for those ecosystems where the vegetation is renewed every year (here an open wetland), seasonal patterns can also be observed in the evergreen ecosystems (here a coniferous forest).

We examined the illumination sensitivity of our digital camera system by analysing the images of a grey reference plate, which was included in the camera view. Limited solar radiation restricts the use of images during the wintertime as well as during the night-time. At our sites in northern Finland, the daytime radiation levels were sufficient for image analysis from February to October. During that period, a diurnal window of 10:00–14:00 (local winter time) provides stable GCC data. Our results show that the variability in cloudiness and solar zenith angle during the daytime does not play a significant role in the GCC analysis. However, it would be relevant to investigate the seasonal dependence of GCC on sun elevation, especially for the coniferous forest.

We observed a clear seasonal GCC cycle at both study sites. At the wetland, GCC correlated well with the daily photosynthetic capacity estimated from the ecosystem–atmosphere flux measurements. The interannual variation in GCC was also consistent with the observed CO_2 exchange and meteorological conditions. At the forest site, the seasonal GCC cycle correlated well with the flux data in 2015 but showed more deviations during the summer of 2014. For

both ecosystems, the correlation between GCC and CO$_2$ exchange was highest during the spring.

In addition to depicting the seasonal course of ecosystem functioning, we showed that GCC responds to environmental changes on a shorter timescale. We observed that at both sites the increase of GCC and photosynthesis ongoing in June was ceased during a 2-week-long cold and wet period. For an unknown reason, the GCC values even slightly decreased during that period. It is possible that such a reduction is an artefact caused by wet surfaces, for example, rather than a response to an actual decrease in the chlorophyll concentration in leaves and needles.

Due to the low cost of the instrumentation involved, phenology monitoring can be established in a much larger number of locations than ecosystem–atmosphere flux measurements, thus providing a wider geographical basis for improvement of the phenological and photosynthesis components of land surface models that need more calibration and validation. The digital repeat images allow the detection of phenological events, such as shoot elongation and the start of needle growth that cannot be obtained from CO$_2$ flux measurements alone. Therefore, they should be utilized to enhance the analysis of flux data. Furthermore, as our results show, the seasonal cycle of different vegetation types within the footprint of the flux measurements can be determined. This could help decompose the integrated CO$_2$ flux observations when the distribution of the vegetation types within the area is known.

5 Data availability

The data presented in this study are provided as a supplement to this article.

The Supplement related to this article is available online at doi:10.5194/gi-5-417-2016-supplement.

Edited by: M. Paton
Reviewed by: three anonymous referees

References

Ahrends, H. E., Etzold, S., Kutsch, W. L., Stoeckli, R., Bruegger, R., Jeanneret, F., Wanner, H., Buchmann, N., and Eugster, W.: Tree phenology and carbon dioxide fluxes: use of digital photography for process-based interpretation at the ecosystem scale, Clim. Res., 39, 261–274, doi:10.3354/cr00811, 2009.

Arneth, A., Harrison, S. P., Zaehle, S., Tsigaridis, K., Menon, S., Bartlein, P. J., Feichter, J., Korhola, A., Kulmala, M., O'Donnell, D., Schurgers, G., Sorvari, S., Vesala, T.: Terrestrial biogeochemical feedbacks in the climate system, Nat. Geosci., 3, 525–532, 2010.

Aurela, M., Tuovinen, J.-P., and Laurila, T.: Net CO$_2$ exchange of a subarctic mountain birch ecosystem, Theor. Appl. Climatol., 70, 135–148, 2001.

Aurela, M., Lohila, A., Tuovinen, J.-P., Hatakka, J., Riutta, T., and Laurila, T.: Carbon dioxide exchange on a northern boreal fen, Boreal Environ. Res., 14, 699–710, 2009.

Baldocchi, D.: Assessing the eddy covariance technique for evaluating carbon dioxide exchange rates of ecosystems: past, present and future, Glob. Change Biol., 9, 479–492, 2003.

Baldocchi, D. D., Black, T. A., Curtis, P. S., Falge, E., Fuentes, J. D., Granier, A., Gu, L., Knohl, A., Pilegaard, K., Schmid, H. P., Valentini, R., Wilson, K., Wofsy, S., Xu, L., and Yamamoto, S.: Predicting the onset of carbon uptake by deciduous forests with soil temperature and climate data: a synthesis of FLUXNET data, Int. J. Biometeorol., 49, 377–387, 2005.

Barr, A. G., Black, T. A., Hogg, E. H., Griffis, T. J., Morgenstern, K., Kljun, N., Theede, A., and Nesic, Z.: Climatic controls on the carbon and water balances of a boreal aspen forest, 1994–2003, Glob. Change Biol., 13, 561–576, 2007.

Bauerle, W. L., Oren, R., Way, D. A., Qian, S. S., Stoy, P. C., Thornton, P. E., Bowden, J. D., Hoffman, F. M., and Reynolds, R. F.: Photoperiodic regulation of the seasonal pattern of photosynthetic capacity and the implications for carbon cycling, P. Natl. Acad. Sci. USA, 109, 8612–8617, 2012.

Berninger, F.: Effects of drought and phenology on GPP in Pinus sylvestris: a simulation study along a geographical gradient, Funct. Ecol., 11, 33–43, 1997.

Black, T. A., Chen, W. J., Barr, A. G., Arain, M. A., Chen, Z., Nesic, Z., Hogg, E. H., Neumann, H. H., and Yang, P. C.: Increased carbon sequestration by a boreal deciduous forest in years with a warm spring, Geophys. Res. Lett., 27, 1271–1274, 2000.

Bryant, R. G. and Baird, A. J.: The spectral behaviour of Sphagnum canopies under varying hydrological conditions, Geophys. Res. Lett., 30, 1134–1138, 2003.

Delbart, N., Picard, G., Le Toans, T., Kergoat, L., Quegan, S., Woodward, I., Dye, D., and Fedotova, V.: Spring phenology in boreal Eurasia over a nearly century time scale, Glob. Change Biol., 14, 603–614, 2008.

Delpierre, N., Dufrene, E., Soudani, K., Ulrich, E., Cecchini, S., Boe, J., and Francois, C.: Modelling interannual and spatial variability of leaf senescence for three deciduous tree species in France, Agr. Forest Meteorol., 149, 938–948, 2009.

Dunn, A. L., Barford, C. C., Wofsy, S. C., Goulden, M. L., and Daube, B. C.: A long-term record of carbon exchange in a boreal black spruce forest: means, responses to interannual variability, and decadal trends, Glob. Change Biol., 13, 577–590, 2007.

Goulden, M. L., Munger, J. W., Fan, S. M., Daube, B. C., and Wofsy, S. C.: Measurements of carbon sequestration by long-term eddy covariance: methods and a critical evaluation of accuracy, Glob. Change Biol., 2, 169–182, 1996.

Ide, R., Nakaji, T., Motohka, T., and Oguma, H.: Advantages of visible-band spectral remote sensing at both satellite and near-surface scales for monitoring the seasonal dynamics of GPP in a Japanese larch forest, J. Agr. Meteorol., 67, 75–84, 2011.

Keeling, C. D., Chin, J. F. S., and Whorf, T. P.: Increased activity of northern vegetation inferred from atmospheric CO_2 measurements, Nature, 382, 146–149, 1996.

Keenan, T. F., Darby, B., Felts, E., Sonnentag, O., Friedl, M., Hufkens, K., O'Keefe, J. F., Klosterman, S., Munger, J. W., Toomey, M., and Richardson, A. D.: Tracking forest phenology and seasonal physiology using digital repeat photography: a critical assessment, Ecol. Appl., 24, 1478–1489, 2014.

Körner, C. and Basler, D.: Warming, photoperiods, and tree phenology response, Science, 329, 278–278, 2010.

Linkosalo, T., Häkkinen, R., Terhivuo, J., Tuomenvirta, H., and Hari, P.: The time series of flowering and leaf bud burst of boreal trees (1846–2005) support the direct temperature observations of climatic warming, Agr. Forest Meteorol., 149, 453–461, 2009.

Migliavacca, M., Galvagno, M., Cremonese, E., Rossini, M., Meroni, M., Sonnentag, O., Manca, G., Diotri, F., Busetto, L., Cescatti, A., Colombo, R., Fava, F., Morra di Cella, U., Pari, E., Siniscalco, C., and Richardson, A.: Using digital repeat photography and eddy covariance data to model grassland phenology and photosynthetic CO_2 uptake, Agr. Forest Meteorol., 151, 1325–1337, 2011.

Migliavacca, M., Sonnentag, O., Keenan, T. F., Cescatti, A., O'Keefe, J., and Richardson, A. D.: On the uncertainty of phenological responses to climate change, and implications for a terrestrial biosphere model, Biogeosciences, 9, 2063–2083, doi:10.5194/bg-9-2063-2012, 2012.

Morisette, J. T., Richardson, A. D., Knapp, A. K., Fisher, J. I., Graham, E. A., Abatzoglou, J., Wilson, B. E., Breshears, D. D., Henebry, G. M., Hanes, J. M., and Liang, L.: Tracking the rhythm of the seasons in the face of global change: Phenological research in the 21st century, Front. Ecol. Environ., 7, 253–260, 2009.

Nordli, O., Wielgolaski, F. E., Bakken, A. K., Hjeltnes, S. H., Mage, F., Sivle, A., and Skre, O.: Regional trends for bud burst and flowering of woody plants in Norway as related to climate change, Int. J. Biometeorol., 52, 625–639, 2008.

Peichl, M., Sonnentag, O., and Nilsson, M. B.: Bringing Color into the Picture: Using Digital Repeat Photography to Investigate Phenology Controls of the Carbon Dioxide Exchange in a Boreal Mire, Ecosystems, 18, 115–131, 2015.

Petach, A., Toomey, M., Aubrecht, D., Richardson, A. D: Monitoring vegetation phenology using an infrared-enabled security camera, Agr. Forest Meteorol., 195, 143–151, 2014.

Pirinen, P., Simola, H., Aalto, J., Kaukoranta, J.-P., Karlsson, P., and Ruuhela, R.: Climatological statistics of Finland 1981–2010, Reports 2012:1, Finnish Meteorological Institute, Helsinki, 2012.

Pudas, E., Leppälä, M., Tolvanen, A., Poikolainen, J., Venäläinen, A., and Kubin, E.: Trends in phenology of Betula pubescens across the boreal zone in Finland, Int. J. Biometeorol., 52, 251–259, 2008.

Reichstein, M., Falge, E., Baldocchi, D., Papale, D., Aubinet, M., Berbigier, P., Bernhofer, C., Buchmann, N., Gilmanov, T., Granier, A., Grünwald, T., Havránková, K., Ilvesniemi, H., Janous, D., Knohl, A., Laurila, T., Lohila, A., Loustau, D., Matteucci, G., Meyers, T., Miglietta, F., Ourcival, J.-M., Pumpanen, J., Rambal, S., Rotenberg, E., Sanz, M., Tenhunen, J., Seufert, G., Vaccari, F., Vesala, T., Yakir, D., and Valentini, R.: On the separation of net ecosystem exchange into assimilation and ecosystem respiration: review and improved algorithm, Glob. Change Biol., 11, 1424–1439, 2005.

Richardson, A. D., Jenkins, J. P., Braswell, B. H., Hollinger, D. Y., Ollinger, S. V., and Smith, M.-L.: Use of digital webcam images to track spring green-up in a deciduous broadleaf forest, Oecologia, 152, 323–334, 2007.

Richardson, A. D., Hollinger, D. Y., Dail, D. B., Lee, J. T., Munger, J. W., and O'Keefe, J.: Influence of spring phenology on seasonal and annual carbon balance in two contrasting New England forests, Tree Physiol., 29, 321–331, 2009.

Richardson, A. D., Keenan, T. F., Migliavacca, M., Ryua, Y., Sonnentag, O., and Toomey, M.: Climate change, phenology, and phenological control of vegetation feedbacks to the climate system, Agr. Forest Meteorol., 169, 156–173, 2013.

Rosenzweig, C., Casassa, G., Karoly, D. J., Imeson, A., Liu, C., Menzel, A., Rawlins, S., Root, T. L., Seguin, B., and Tryjanowski, P.: Supplementary material to chapter 1: Assessment of observed changes and responses in natural and managed systems. Climate Change 2007: Impacts, Adaptation and Vulnerability. Contribution of Working Group II to the Fourth Assessment Report of the Intergovernmental Panel on Climate Change, edited by: Parry, M. L., Canziani, O. F., Palutikof, J. P., van der Linden, P. J., and Hanson, C. E., Cambridge University Press, Cambridge, UK, 2007

Sonnentag, O., Detto, M., Vargas, R., Ryu, Y., Runkle, B. R. K., Kelly, M., and Baldocchi, D. D.: Tracking the structural and functional development of a perennial pepperweed (*Lepidium latifolium* L.) infestation using a multi-year archive of webcam imagery and eddy covariance measurements, Agr. Forest Meteorol., 151, 916–926, 2011.

Sonnentag, O., Hufkens, K., Teshera-Sterne, C., Young, A. M., Friedl, M., Braswell, B. H., Milliman, T., O'Keefe, J., and Richardson, A. D.: Digital repeat photography for phenological research in forest ecosystems, Agr. Forest Meteorol., 152, 159–177, 2012.

Tanis, C. M. and Arslan, A. N.: FMIPROT – Finnish Meteorological Institute Image Processing Tool, User manual, available at: http://monimet.fmi.fi/index.php?style=warm&page=FMIPROT, 2016.

Tanja, S., Berninger, F., Vesala, T., Markkanen, T., Hari, P., Mäkelä, A., Ilvesniemi, H., Hänninen, H., Nikinmaa, E., Huttula, T., Laurila, T., Aurela, M., Grelle, A., Lindroth, A., Arneth, A., Shibistova, O., and Lloyd, J.: Air temperature triggers the recovery of evergreen boreal forest photosynthesis in spring, Glob. Change Biol., 9, 1410–1426, 2003.

Toomey, M., Friedl, M., Frolking, S., Hufkens, K., Klosterman, S., Sonnentag, O., Baldocchi, D., Bernacchi, C., Biraud, S. C., Bohrer, G., Brzostek, E., Burns, S. P., Coursolle, C., Hollinger, D. Y., Margolis, H. A., McCaughey, H., Monson, R. K., Munger, J. W., Pallardy, S., Phillips, R. P., Torn, M. S., Wharton, S., Zeri, M., and Richardson, A. D.: Greenness indices from digital cameras predict the timing and seasonal dynamics of canopy-scale photosynthesis, Ecol. Appl., 25, 99–115, 2015.

Vesala, T., Suni, T., Rannik, Ü., Keronen, P., Markkanen, T., Sevanto, S., Grönholm, T., Smolander, S., Kulmala, M., Ilvesniemi, H., Ojansuu, R., Uotila, A., Levula, J., Mäkelä, A., Pumpanen, J., Kolari, P., Kulmala, L., Altimir, N., Berninger, F., Nikinmaa, E., and Hari, P.: Effect of thinning on surface fluxes in a boreal forest, Global Biogeochem. Cy., 19, GB2001, doi:10.1029/2004GB002316, 2005.

White, M. A. and Nemani, R. R.: Canopy duration has little influence on annual carbon storage in the deciduous broadleaf forest, Glob. Change Biol., 9, 967–972, 2003.

Wingate, L., Ogée, J., Cremonese, E., Filippa, G., Mizunuma, T., Migliavacca, M., Moisy, C., Wilkinson, M., Moureaux, C., Wohlfahrt, G., Hammerle, A., Hörtnagl, L., Gimeno, C., Porcar-Castell, A., Galvagno, M., Nakaji, T., Morison, J., Kolle, O., Knohl, A., Kutsch, W., Kolari, P., Nikinmaa, E., Ibrom, A., Gielen, B., Eugster, W., Balzarolo, M., Papale, D., Klumpp, K., Köstner, B., Grünwald, T., Joffre, R., Ourcival, J.-M., Hellstrom, M., Lindroth, A., George, C., Longdoz, B., Genty, B., Levula, J., Heinesch, B., Sprintsin, M., Yakir, D., Manise, T., Guyon, D., Ahrends, H., Plaza-Aguilar, A., Guan, J. H., and Grace, J.: Interpreting canopy development and physiology using a European phenology camera network at flux sites, Biogeosciences, 12, 5995–6015, doi:10.5194/bg-12-5995-2015, 2015.